RHEA'S INTERNAL STRUCTURE INFERRED FROM CASSINI GRAVITY AND TOPOGRAPHY

Doug Hemingway[1] (djheming@ucsc.edu), Francis Nimmo[1], Paolo Tortora[2], Marco Zannoni[2], Luciano Iess[3], Marzia Parisi[3], and Peter Thomas[4]. [1]Department of Earth & Planetary Sciences, University of California Santa Cruz, 1156 High Street, Santa Cruz, California, 95064, USA, [2]Dipartimento di Ingegneria Industriale, Università di Bologna, Forlì, Italy, [3]Dipartimento di Ingegneria Meccanica e Aerospaziale, Sapienza Università di Roma, Rome, Italy, [4]Department of Astronomy, Cornell University, Ithaca, New York, USA.

Summary: Combined analyses of gravity and topography can yield useful information about the interior structures of planetary bodies [1–4]. Based on radio tracking of the *Cassini* spacecraft, we present an estimate of the gravity field of Saturn's large moon Rhea. Combining this with a shape model based on limb profile analyses, we attempt to constrain Rhea's internal structure, concluding that the core likely exhibits some excess flattening.

Gravity: During its time in the Saturn system, *Cassini* has performed two close fly-bys of Rhea devoted to gravity investigations: one in November 2005, and another in March 2013. As in previous work [2,4,5], the gravity field of Rhea was estimated by reconstructing the spacecraft trajectory during these encounters, making use of precise measurements of the Doppler shift of a highly stable microwave radio link between *Cassini* and the ground station antennas of NASA's Deep Space Network.

The available data were analyzed in a multi-arc fit estimating a fully unconstrained quadrupole gravity field for Rhea, the Rhea state vector at a reference epoch, and the spacecraft initial state vector for each fly-by. The stability of the solutions was tested by perturbing the dynamical model in various ways, including estimating a full 4x4 gravity field and changing the *a priori* uncertainties.

The resulting estimate of Rhea's gravity field exhibits a statistically significant departure from the hydrostatic expectation (Figure 1), with a J_2/C_{22} ratio of 3.9±0.1 (the hydrostatic ratio is ~3.33). As a result, the moment of inertia cannot be inferred directly from the Radau-Darwin approximation. Estimating the moment of inertia directly from the J_2 or C_{22} coefficients yields incompatible and unrealistic estimates of ~0.41 and ~0.37, respectively.

Shape: Rhea's shape has been determined previously via analyses of limb profiles [6,7]. After incorporating the latest available data, we repeat this analysis, obtaining a best-fitting tri-axial ellipsoid with semi-axes:

$a = 765.7 \pm 0.3$ km,
$b = 763.6 \pm 0.3$ km,
$c = 762.9 \pm 0.2$ km,

from which we obtain the unnormalized degree-2 coefficients: $J_2 = 1190 \pm 260$ m, $C_{22} = 350 \pm 120$ m

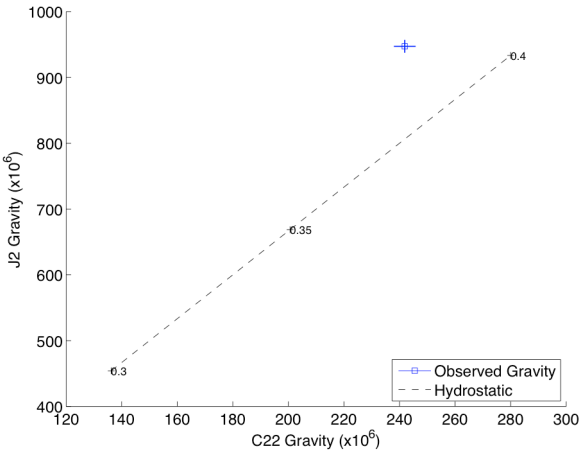

Figure 1: J_2 and C_{22} dimensionless gravitational potential coefficients for Rhea, with crosshairs illustrating the one-sigma uncertainties. Expected hydrostatic values of J_2 and C_{22} are indicated for various normalized moments of inertia along the theoretical hydrostatic line (dashed line).

(uncertainties are all one-sigma). Figure 2 illustrates how the shape compares with the hydrostatic expectation for various assumed moments of inertia. The central value is close to the expectation for a nearly homogeneous, hydrostatic body, however the uncertainties are large.

Internal Structure: There are a number of ways to explain the excess oblateness (higher than expected J_2/C_{22} ratio) in Rhea's gravity field that are consistent with the observed shape.

Homogeneous Model: If Rhea is of uniform density, it can be shown [8,3,4] that the shape required to explain the observed gravity is given by

$$H_{lm} = \frac{(2l+1)R}{3} G_{lm} \qquad (1)$$

where R is Rhea's mean radius, and G_{lm} and H_{lm} are spherical harmonic coefficients of degree l and order m, representing the dimensionless gravitational potential and topography, respectively. In addition to the J_2 and C_{22} values estimated from limb profile observations, Figure 2 shows the values obtained from equation (1) based on the gravity coefficients illustrated in Figure 1. The gravity field is thus consistent with a homogeneous Rhea of the observed shape, to within the shape model's uncertainties.

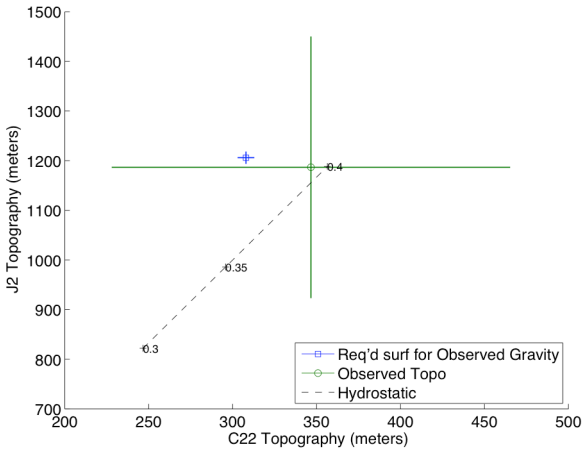

Figure 2: Limb-profile-based estimates of the J_2 and C_{22} topography coefficients for Rhea, with crosshairs illustrating the one-sigma uncertainties. Also shown is the surface topography required for a homogeneous Rhea to produce the observed gravity field, computed from equation (1).

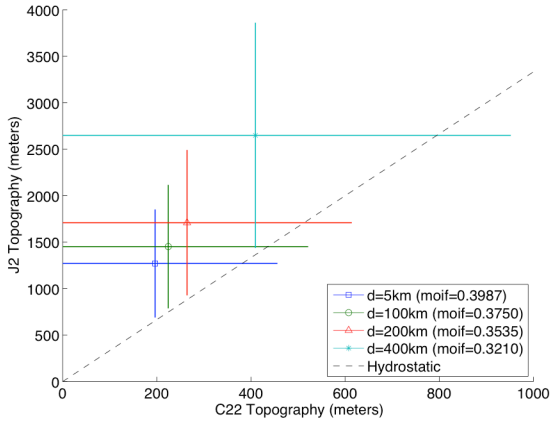

Figure 3: Required J_2 and C_{22} core-mantle-boundary topography for each of four different mantle thicknesses (5, 100, 200, & 400 km) relative to the expected hydrostatic line (dashed black line), assuming the surface conforms to our shape model. For each assumed mantle thickness, the corresponding moment of inertia factor is given in the legend.

Two-Layer Model: Considering that the surface is most likely water ice [9,10], it may be more realistic to assume some internal layering. Here, we consider a simple two-layer model: silicate core and H_2O mantle. We assume the density of the mantle is 920 kg/m^3 and we examine a series of different core densities. For each assumed core density, we compute the core radius required to satisfy the observed bulk density constraint ($\bar{\rho}$ = 1236 kg/m^3).

If the surface conforms closely to the central values of our shape model, then the excess oblateness of the gravity field requires an irregular core shape (i.e., oblateness at the core-mantle-boundary that is beyond the hydrostatic expectation)—similar concepts have been considered previously for Enceladus [6,11] and Mimas [12]. With this two-layer model, we can solve for the core-mantle-boundary topography required to give rise to the observed gravity field (e.g., [11,13]). Given a known gravity field and surface topography, expressed in spherical harmonics, it can be shown that the required topography at the core-mantle-boundary is given by

$$H_{lm}^{cmb} = \frac{1}{\Delta\rho}\left(\frac{R}{R-d}\right)^{l+2}\left[\frac{(2l+1)R\bar{\rho}}{3}G_{lm} - \rho_s H_{lm}^{s}\right] \quad (2)$$

where H_{lm}^{cmb} is the core-mantle-boundary topography at degree l and order m, $\Delta\rho$ is the density contrast at the core-mantle-boundary, d is the depth of the core-mantle-boundary ($d = R - R_{core}$), $\bar{\rho}$ is Rhea's bulk density, R is Rhea's full radius, ρ_s is the density of the mantle, G_{lm} is the dimensionless gravitational potential resolved at radius R, and H_{lm}^{s} is the surface topography.

As illustrated in Figure 3, if the surface conforms to our shape model (Figure 2), and assuming we have not significantly overestimated the C_{22} topography, then some excess core oblateness (roughly 1 km) is required to account for the observed gravity field. This excess core topography implies stresses of ~0.3 MPa, which are readily supported by cold silicate materials. With larger mantle thicknesses, the core-mantle-boundary is deeper and so larger amplitudes are required to overcome the resulting attenuation of the gravity signal.

Conclusions: The observed shape is consistent with the shape required for an undifferentiated (uniform density) Rhea to account for the observed gravity. However, because the surface is more likely to be water ice, a two-layer model may be a better approximation (*cf.* [5]). In this case, and assuming a mantle density of 920 kg/m^3, some ~1 km of excess core oblateness may be necessary to account for the observed gravity (Figure 3). A wide range of moments of inertia is allowed, but models with low moments of inertia (i.e., more differentiation) require greater magnitudes of excess core topography to satisfy the observations.

References: 1.Wieczorek, M. A. in *Treatise Geophys.* **10,** 165–206 (2007). 2. Iess, L. *et al. Science* **327,** 1367–9 (2010). 3. Hemingway, D., *et al. Nature* **500,** 550–552 (2013). 4. Iess, L. *et al. Science* **344,** 78–80 (2014). 5. Anderson, J. D. & Schubert, G. *Geophys. Res. Lett.* **34,** L02202 (2007). 6. Thomas, P. *et al. Icarus* **190,** 573–584 (2007). 7. Nimmo, F., Bills, B. G. & Thomas, P. C. *J. Geophys. Res.* **116,** E11001 (2011). 8. Jeffreys, H. (Cambridge University Press, 1976). 9. Clark, R. N. & Owensby, P. D. The infrared spectrum of Rhea. *Icarus* **46,** 354–360 (1981). 10. Stephan, K. *et al. Planet. Space Sci.* **61,** 142–160 (2012). 11. McKinnon, W. B. *J. Geophys. Res. Planets* **118,** n/a–n/a (2013). 12. Tajeddine, R. *et al. Science (80-.).* **346,** 322–324 (2014). 13. Lefevre, A., *et al. Icarus* (2014)